RESEARCH ARTICLE | JANUARY 17 2024

Studying fast-ion populations using oscillations in solid-state neutral-particle analyzer signal and neutral-beam injection power ⊘

E. Parr ✉ ⓘ ; K. G. McClements ⓘ ; W. W. Heidbrink ⓘ ; C. A. Michael ⓘ ; G. Prechel ⓘ ;
J. F. Rivero-Rodriguez ⓘ ; MAST-U Team

Check for updates

View Online   Export Citation   CrossMark

AIP Publishing

Studying fast-ion populations using oscillations in solid-state neutral-particle analyzer signal and neutral-beam injection power

View Online   Export Citation   CrossMark

E. Parr,[1,a] (ID) K. G. McClements,[1] (ID) W. W. Heidbrink,[2] (ID) C. A. Michael,[3] (ID) G. Prechel,[2] (ID)
J. F. Rivero-Rodriguez,[1] (ID) and MAST-U Team[b]

AFFILIATIONS

[1] UKAEA, Culham Science Centre, Oxfordshire OX14 3DB, United Kingdom
[2] University of California Irvine, Irvine, California 92697, USA
[3] University of California, Los Angeles, California 90095, USA

[a] Author to whom correspondence should be addressed: edward.parr@ukaea.uk
[b] See author list of J. R. Harrison *et al.*, Nucl. Fusion **59**, 112011 (2019).

ABSTRACT

A method for determining the fast-ion population density in magnetically confined plasmas as a function of pitch-radius, (λ, R), using a solid-state neutral-particle analyzer (ssNPA) signal and neutral-beam injection (NBI) power-output data has been developed. Oscillations in the NBI power output are replicated only in the *active* part of the ssNPA signal, allowing this to be separated from the *passive* and background signals, which usually complicate data from this diagnostic. Results obtained using this method are compared with those from standard techniques using data from the Mega-Amp Spherical Tokamak Upgrade spherical tokamak.

Published under an exclusive license by AIP Publishing. https://doi.org/10.1063/5.0178179

I. INTRODUCTION

Fast-ion (FI) populations in magnetically confined plasmas are key to plasma heating and, in the case of fast ions introduced through neutral beams, plasma current drive as well. Redistribution and loss of these fast ions, however, may be caused by instabilities in the plasma, many of which are driven by the fast ions themselves. It is, therefore, vital to understand the distribution and evolution of these populations in order to produce high-performance magnetically confined fusion plasmas.

One type of diagnostic tool that is used in the study of fast ions is the solid-state neutral-particle analyzer (ssNPA).[1–9] These devices measure fast-ion populations via the fast-neutral (FN) fluxes produced following charge-exchange (CX) with neutrals (e.g., in deuterium plasmas: $D_{FI}^+ + D^0 \rightarrow D_{FN}^0 + D^+$). As CX involves negligible momentum transfer and the fast neutrals subsequently escape the plasma unperturbed in straight-line trajectories, all of the velocity information of the preceding fast ion is preserved. As an *active* diagnostic, the ssNPA relies on neutrals from neutral-beam injection (NBI) heating systems to induce CX. Compact silicon photo-diodes

used in ssNPA diagnostics allow multiple lines-of-sight to be established, intersecting the neutral beam at various pitch, λ (the ratio of the ion velocity parallel to, and in the direction of, the magnetic field, $v_\parallel$, and the total, v_{total}), and major radii, R. Considering the fast-ion population density distribution in velocity space coordinates, $f_{FI}(R, z, \lambda, E, t)$, ssNPA diagnostics allow for a particular slice of this distribution—with respect to (λ, R)—to be measured. Here, z is the vertical spatial coordinate, defined with respect to the plane in which the lines of sight lie (normally, this is the geometric mid-plane of the device). Use of the ssNPA in current mode[3,4,7–9] produces a voltage output, S, which is in principle, proportional to the rate of the incoming fast-neutral flux, irrespective of energy, E. The portion of the fast-ion energy distribution that may be measured by the ssNPA in the current mode is, therefore, integral to the transmission efficiency, ε_n, for neutrals in the detector,

$$N_{FI} = \int \varepsilon_n(E) \cdot f_{FI}(E) \cdot dE. \tag{1}$$

Here, the detector efficiency effectively gives a threshold energy for fast-ion measurement, which is determined by the material

17 January 2024 13:52:57

and thickness of the filter used. The use of different filter thicknesses for detectors with the same line of sight can also be used to offer some information on the fast-ion energy distribution. The loss in energy-spectroscopy capabilities of the current mode is countered by excellent time resolution. In the Mega-Amp Spherical Tokamak Upgrade (MAST-U), fast-ion populations have been studied using ssNPA data at 2 μs intervals.[9] This is particularly useful in the study of fast-ion redistribution and loss following instabilities that occur on relatively short time-scales, such as sawteeth.

One issue, however, with using active diagnostics such as the ssNPA is that the neutrals that induce CX in fast ions are not only provided by the NBI but are present as a background minority species in the plasma. The signal produced from CX between fast ions and these background neutrals, the so-called *passive* signal (S_p), is then measured together with the desired *active* signal, produced from CX with NBI neutrals (S_a). This can greatly complicate ssNPA results, as the fast-ion population densities producing signals are no longer only those of the $N_{FI}(\lambda, R)$ slice at the points of line-of-sight and NBI intersection. One solution to the problem of separating these signal components is the use of a second diagnostic performing a passive measurement, toroidally displaced from the first, for which the line-of-sight does not intersect the NBI.[4,7,10] The magnitude of the passive signal may then be estimated and subtracted from the total to give just the active contribution, assuming toroidal symmetry in the background neutral density. This method, however, introduces additional uncertainties into the measurements and can be complicated by different sources of background signal in the diagnostic lines of sight. Another method utilizes *beam notching*, whereby the NBI is switched off for short periods at set intervals during the pulse. The passive and background signal components may then be ascertained in the absence of the beam and subtracted from the total signal immediately preceding the switch-off to determine the active component. However, the timing of the beam notches must be pre-set and, in MAST-U, have a minimum duration of ~10 ms. It is, therefore, not a suitable method for studying the redistribution and loss of fast ions following instabilities, which are often unpredictable and short-lived. In addition, the NBI populates the fast-ion distribution, which drives many of the instabilities. The periodic switch-off of the beam will inevitably, therefore, affect the nature and frequency of the very events that are intended to be studied.

One alternative solution to separating the active and passive signals measured with ssNPA diagnostics, which will be presently described, is to utilize oscillations in the power output of the NBI. These oscillations are replicated only in the active part of the ssNPA signal, which is proportional to both the NBI power output—proportional to the density of neutrals provided by the NBI at a given time, assuming a constant acceleration voltage—and the fast-ion density at the point of the NBI and ssNPA line-of-sight intersection. The amplitude of the oscillations produced in a ssNPA signal relative to those of the NBI power output is, therefore, indicative of the fast-ion population density, $N_{FI}(\lambda, R)$.

II. ANALYSIS METHOD

The active part of the ssNPA signal in current mode, S_a, may be expressed as

$$S_a = A \cdot \Sigma_{CX} \cdot N_{NBI} \cdot N_{FI}, \tag{2}$$

where N_{NBI} is the neutral density provided by the NBI and N_{FI} is the fast-ion population density with (λ, R), both at the point of line-of-sight and NBI intersection, Σ_{CX} is a coefficient containing the integrated CX cross-sections for the fast-ion energy distribution, and A embodies the overall response of the system. If an oscillation is applied to the NBI power output, δP_{NBI}, each of the terms in Eq. (2) may then be expressed as the sum of a time-averaged component, e.g., $\bar{S}_a$, and an oscillatory component, δS_a. For small power-output modulations driven only by changes to the beam current, the second-order oscillatory terms, as well as those associated with the A and Σ_{CX} terms, may be neglected, giving

$$S_a = \bar{S}_a + \delta S_a = A \cdot \Sigma_{CX} \cdot (\bar{N}_{NBI}\bar{N}_{FI} + \bar{N}_{FI}\delta N_{NBI} + \bar{N}_{NBI}\delta N_{FI}), \tag{3}$$

and when considering only the oscillating part of the active signal,

$$\delta S_a = A \cdot \Sigma_{CX} \cdot (\bar{N}_{FI}\delta N_{NBI} + \bar{N}_{NBI}\delta N_{FI}). \tag{4}$$

Considering the $\bar{N}_{NBI}\delta N_{FI}$ term, this represents the oscillatory contribution from modulations in the fast-ion population driven by those of the NBI power output. Assuming that the slowing-down time scales for the portion of the fast-ion population being measured are considerably longer than those of the NBI power-output oscillations, then the $\bar{N}_{NBI}\delta N_{FI}$ term may be neglected. Assuming Σ_{CX} and A remain constant and no oscillations are present in the passive or background signal components, then the fast-ion population density may be given (in suitably rescaled units) by the rate of change of S with respect to N_{NBI},

$$N_{FI} = \frac{\delta S}{\delta N_{NBI}}. \tag{5}$$

Some of the assumptions made earlier are to some extent, borne out by data from MAST-U. Figure 1(a) shows oscillations that occur in the power output of the South-South (SS) NBI, with panel (b) showing a corresponding ssNPA signal output, S. The NBI power output is given as the product of the measured extracted current and voltage, with subsequent neutralization and transmission efficiencies included. It should be noted that the oscillations in the NBI power output on MAST-U derive almost entirely from fluctuations in the NBI current; the voltage over which the neutrals are accelerated is stable to ~±0.5%. The NBI(SS) beam intersects the ssNPA lines-of-sight at the mid-plane of MAST-U, producing an active signal. Here, the NBI(SS) power oscillations are clearly imprinted in the ssNPA signal, as expected. This may then be compared with equivalent data from the South-West (SW) NBI in MAST-U, which has a beam trajectory above the machine mid-plane and, therefore, does not intersect the ssNPA lines-of-sight, as shown in Fig. 2(a), with ssNPA data in panel (b). The ssNPA signals measured during NBI(SW) heating [without NBI(SS)] are produced by passive contributions and background only, the latter mainly deriving from x rays with photon energy $E_\gamma \gtrsim 1.5$ keV.[7] As no oscillations in this case are observed in S, we may assume that the beam modulations are replicated only in the active signal, i.e., $\delta S = \delta S_a$. Furthermore, as a non-zero δN_{FI} term would be expected to produce oscillations in the passive signal, which are not observed, its neglect in Eq. (5) also appears justified. This gives confidence in the assumption that
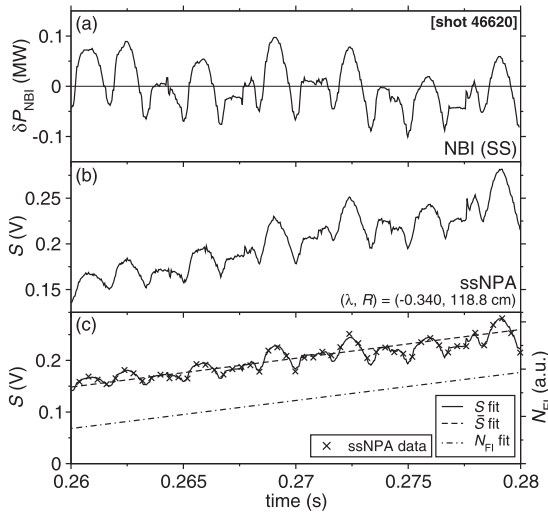
FIG. 1. Time traces from MAST-U shot number 46 620. Panel (a) shows the NBI(SS) power-output oscillations, δP_{NBI}, and panel (b) the ssNPA signal, S, from the line-of-sight intersection with NBI(SS) at $(\lambda, R) = (-0.340, 118.8 \text{ cm})$. Panel (c) shows the same ssNPA data, represented as crosses, giving one in ten data points, along with the results of the fit to Eq. (7): the total fitted function, $S(t, \delta N_{NBI})$, shown as a solid line; the smoothly varying time-averaged rate, $\bar{S}(t)$, shown as a dashed line; and the fast-ion population density, $N_{FI}(t)$, shown as a dotted–dashed line. The latter two variables were fitted as linear functions with respect to time.
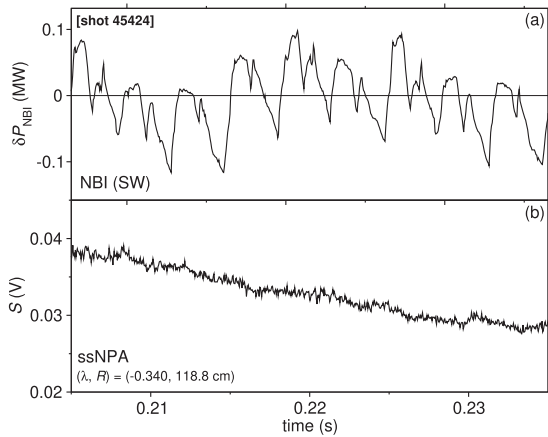
FIG. 2. Time traces from MAST-U shot number 45 424. Panel (a) shows the NBI(SW) power-output oscillations, δP_{NBI}, and panel (b) the ssNPA rate, S, from the detector, which would have line-of-sight intersection with NBI(SS) at $(\lambda, R) = (-0.340, 118.8 \text{ cm})$.

the oscillations in S derive directly and solely from those of the NBI-produced neutral density, without a contribution from fluctuations in the fast-ion density population or any other term in Eq. (2).

As the N_{FI} that determines the passive signal is predominantly that which exists at the edge of the plasma, it is also important to investigate the possible presence of a δN_{FI} term across the whole plasma profile. For this, fast-ion diagnostics, in which the signal is dependent only on the fast-ion density, and not the neutral density

may be used. Two such diagnostics at MAST-U are the fission chamber[11] and the neutron camera,[12] which measure the neutron rates produced following D–D fusion reactions with time resolutions of 1 μs and 1 ms, respectively. These rates are a proxy for fast-ion densities and are measured globally and from collimated line integrations, respectively. The observed absence of any oscillations in the signals from either of these diagnostics during SS or SW NBI heating is consistent with fast-ion populations across the whole of the plasma that do not fluctuate with δP_{NBI}.

Using this framework of assumptions, a method to measure the fast-ion population density from ssNPA-signal and NBI power-output data may be devised. For measured ssNPA data, the total signal, S, can be separated into a time-averaged total component, $\bar{S}$, resulting from the active, passive, and background signals, and an oscillatory component present only in the active part of the signal,

$$S(t) = \bar{S}(t) + \delta S(t). \tag{6}$$

These oscillations, δS, may be given as those of the NBI neutral density, δN_{NBI}, scaled to N_{FI}, as in Eq. (5),

$$S(t, \delta N_{NBI}) = \bar{S}(t) + [N_{FI}(t) \cdot \delta N_{NBI}]. \tag{7}$$

The neutral-density oscillations may be given as those of the NBI power output scaled by a factor, $C(x, y)$, which corrects for beam intensity losses along the beamline in the toroidal x–y plane using Thomson-scattering data of the electron-density profile[13] and the width of beam subtended by each line-of-sight,

$$\delta N_{NBI} = C(x, y) \cdot \delta P_{NBI}. \tag{8}$$

This, again, assumes that the NBI-power oscillations, δP_{NBI}, derive entirely from the oscillations of the NBI current. When fitting ssNPA data using Eq. (7), the oscillations of the neutral density, δN_{NBI}, represent a second independent variable, and appropriate functions with respect to time should be used for $\bar{S}(t)$ and $N_{FI}(t)$.

III. APPLICATION OF METHOD

The ssNPA on MAST-U[9] consists of three arrays, each with a tungsten filter of different thicknesses (100, 200, and 300 nm). Each array then consists of 15 silicon photodiode detectors, providing 15 separate lines of sight. These three arrays transmit neutrals with an efficiency distribution that reaches 50% (indicating the rough threshold energy) at $E \simeq 18$, 38, and 58 keV, respectively, as calculated using the stopping and range of ions in matter (SRIM) software.[14] The same lines-of-sight and NBI(SS) interaction points are replicated in each of the three arrays, intended to provide information on the fast-ion population energy distribution. The data used for the results presented throughout this publication derive only from the array with a filter thickness of 100 nm.

The present method was applied to NBI power-output and ssNPA data taken from MAST-U shot 46 620 between 260 and 280 ms [shown in Figs. 1(a) and 1(b), the latter for $(\lambda, R) = (-0.340, 118.8 \text{ cm})$]. Results were obtained by fitting the data using Eq. (7), where $\bar{S}(t)$ and $N_{FI}(t)$ varied linearly with time; the results of the fit are given in Fig. 1(c). Figure 3 shows the resulting fast-ion population densities, $N_{FI}(\lambda, R)$, taken at shot times $t = 260$ and 280 ms. Corrections for the inherent efficiency of the diagnostic set-up, determined using soft x-ray intensity measurements, have been
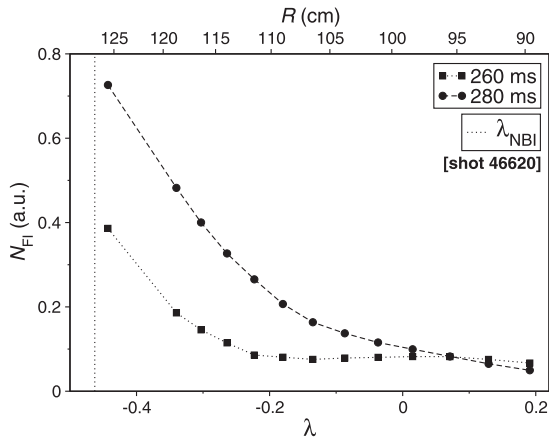
FIG. 3. Fast-ion population densities, N_{FI}, as a function of pitch, λ, and major radius, R, determined using the method presently described from ssNPA-signal and NBI(SS) power-output data. Results taken from MAST-U shot 46 620 and shown for times $t = 260$ and 280 ms. The maximum pitch at which fast ions are deposited by the NBI, λ_{NBI}, at $R = 125.5$ cm (corresponding to the lowest pitch measurement by a detector: $\lambda = -0.443$) is also shown, assuming a mid-plane beam diameter of 25 cm.

FIG. 4. Time traces from MAST-U shot 46 620. Panel (a) shows the NBI(SS) power output and panels (b)–(d) the ssNPA rates, S, from the line-of-sight intersections with NBI at $(\lambda, R) = (-0.340, 118.8$ cm$)$, $(-0.223, 111.6$ cm$)$, and $(+0.015, 98.3$ cm$)$ and approximate passive pitch $\lambda_p = -0.29, -0.18$, and $+0.01$ at $R_{separatrix}$ ~130–140 cm, respectively. The times at which N_{FI} and N'_{FI} have been calculated are indicated in panel (d) with the corresponding symbols used in Fig. 5 and labeled (i)–(v).

applied, as is the case for all results presented in this publication. In addition, shown is the maximum pitch at which fast ions are deposited by the NBI in the plasma via CX at $R = 125.5$ cm (corresponding to the lowest pitch measured by a detector: $\lambda = -0.443$), assuming a mid-plane beam diameter of 25 cm. It should be noted that the fast-ion deposition pitch at all other R values measured by the detectors is lower than that shown for $R = 125.5$ cm.
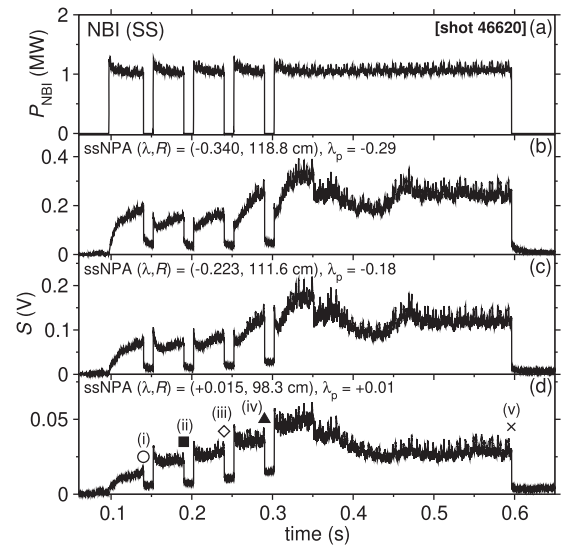
As the NBI heats the plasma (beginning at $t = 250$ ms), the results illustrate how the fast-ion distribution is populated over these 20 ms, with larger increases in N_{FI} seen for (λ, R) values closer to the injection pitch. Increasing N_{FI} may be seen in the increasing amplitude of the ssNPA signal oscillations, relative to those of the NBI(SS) power output, in Fig. 1. The proportional changes in N_{FI} over this time period do not correspond to the respective increases in S values. This is due to the latter, including the unknown contributions of passive and background signals.

A. Comparison with *beam-notching* method

The present method for determining N_{FI} may be compared with the more established *beam-notching* technique.[9] In this method, the combined passive and background contributions to the ssNPA signal, $S_{p+bkr.}$, for an NBI-heated plasma are determined by switching off the NBI for short periods, or notches, removing the active signal. The signal measured during this switch-off then consists of only passive and background contributions and may be subtracted from the total signal, S, immediately preceding the switch-off to estimate the active part alone. The fast-ion population density determined using the beam-notching method may be given as

$$N'_{FI} = (S - S_{p+bkr.})/\bar{N}_{NBI}, \tag{9}$$

where $\bar{N}_{NBI}$ is the NBI neutral density [found from P_{NBI} using the $C(x, y)$ correction coefficients of Eq. (8)] averaged for the time period

over which S is measured. This neutral-density correction is applied to compensate for variations in P_{NBI} over both long time periods and short-term oscillations. Here, again, the CX cross-section coefficient, Σ_{CX}, is assumed to remain constant.

Figure 4 shows time traces from MAST-U shot 46 620, where the beam-notching technique has been applied. The NBI(SS) power-output time-trace [panel (a)] shows four notches of 12 ms at $t = 140, 190, 240$, and 290 ms, preceding each of which N'_{FI} may be determined. The ssNPA-signal traces for active-CX radii-pitch $(\lambda, R) = (-0.340, 118.8$ cm$)$, $(-0.223, 111.6$ cm$)$, and $(+0.015, 98.3$ cm$)$ are shown in panels (b)–(d), with the times at which the active signal may be determined indicated as (i)–(v) on the lower panel; the final beam-off time $(t = 596$ ms$)$ is also highlighted, as the active signal may be determined here in the same way. As discussed, the passive ssNPA signal derives from the CX of fast ions with background neutrals in the plasma. These background neutrals are heavily concentrated at the separatrix, causing the passive signal to be essentially a measure of the pitch distribution of fast ions at the plasma edge. The mid-plane separatrix is measured to be at $R_{separatrix} = 130–140$ cm throughout the beam-notching periods of the shot, giving pitch values measured by the passive signal of $\lambda_p = -0.29, -0.18$, and $+0.01$ for the traces in panels (b)–(d), respectively.

Figure 5(a) compares the results of fast-ion population densities found using the present method, N_{FI} (a), and the beam-notching method, N'_{FI} (b), for the five beam-off points in the shot. Panel (c) gives the ratio between the population densities found using these methods. Both N_{FI} and N'_{FI} values were determined using the same
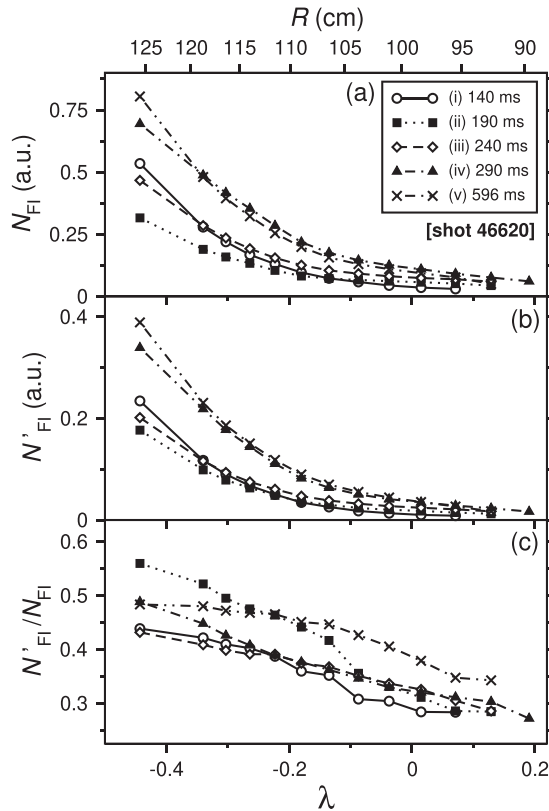
FIG. 5. Comparison of N_{FI} (a) and N'_{FI} (b) values as a function of (λ, R) using the present and beam-notching methods, respectively, for data from MAST-U shot 46 620 at times 140, 190, 240, 290, and 596 ms. Comparisons are made between the two sets of results in panel (c), which gives the ratios of the values, N'_{FI}/N_{FI}.

2.2 ms ranges of S data taken immediately preceding the beam-off times. Fits for $\bar{S}$ changing linearly and N_{FI} remaining constant as functions of time were applied. For N'_{FI}, values of $S_{p+bkr.}$ were estimated using 600 μs ranges of S data following beam-off. $S_{p+bkr.}$ signals were fitted linearly with time and values taken at the point of beam-off.

Comparing these results, the overall characteristics of the N_{FI} and N'_{FI} distributions are similar. However, a gradual reduction in N'_{FI} relative to N_{FI} is observed with increasing λ. This is thought to be due to the non-linearity of the ssNPA output signal at low fast-neutral flux rates. The N_{FI} values are determined from δS measurements, which are taken over smaller voltage ranges than the $S - S_{p+bkr.}$ measurements used for N'_{FI}. Non-linearity at lower voltages could, therefore, lead to lower measured values of N'_{FI} compared with N_{FI}, a discrepancy that would, in this case, increase with λ as the output voltages being measured decreased. The present method appears, therefore, to mitigate the effects of any non-linearity in S measurements using ssNPA diagnostics in the current mode. In addition, the effect of any offset in S and P_{NBI} outputs is removed in the N_{FI} measurements; offsets in the latter contribute to shifts between the N'_{FI}/N_{FI} distributions of values taken at different times.

B. Changes in fast-ion population densities following plasma events

In order to understand how the fast-ion population is affected by plasma instabilities and how these populations may also influence instabilities, the measurement of N_{FI} prior to and following these events is invaluable. In this respect, the beam-notching method is of little use, owing to the unpredictable nature of instabilities and the relatively long time scales in which the NBI notch must be implemented to measure what are often short-lived phenomena. Application of the present method, by contrast, allows for the fast-ion population to be measured throughout the time in which the active-signal inducing NBI is heating the plasma. N_{FI} may, therefore, be measured immediately before and after instability events, with the relative change given as

$$\Delta N_{FI} = \frac{N_{FI}(post) - N_{FI}(pre)}{N_{FI}(pre)}. \tag{10}$$

Here, *pre* and *post* refer to the fast-ion population densities before and after an event. Conventionally, changes in fast-ion populations following instability events have been studied using the total ssNPA signal, S.[15] The relative changes to this, ΔS, can then be calculated as in Eq. (10) using total S values instead of N_{FI}.

Figure 6 shows time traces corresponding to a sawtooth event identified in MAST-U shot 47 127. Sawteeth are characterized by dramatic crashes in temperature and fast-ion population at the plasma core as flux surfaces in that region with safety factor $q \leq 1$ undergo magnetic reconnection. A sharp reduction in the overall
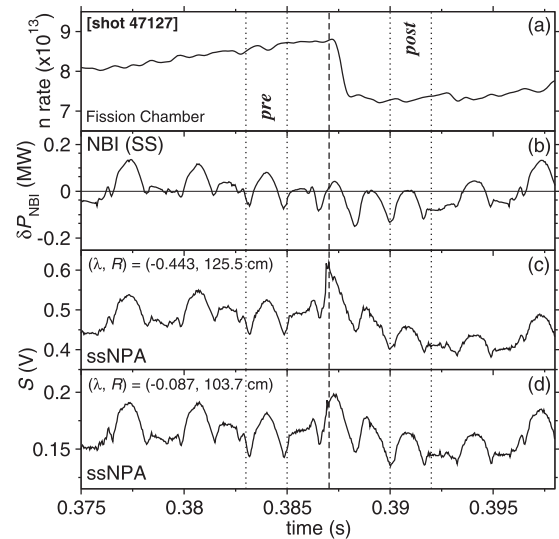
FIG. 6. Time traces indicative of a sawtooth event from MAST-U shot number 47 127. Panel (a) shows the neutron rate measured by the fission chamber. Panel (b) shows the NBI(SS) power-output oscillations, δP_{NBI}, and panels (c) and (d) show the ssNPA signal, S, from the line-of-sight intersection with NBI at (λ, R) = (-0.443, 125.5 cm) and (-0.087, 103.7 cm), respectively. The vertical dashed line indicates the approximate time of the identified sawtooth event, as observed in the ssNPA time-traces, and the vertical dotted lines show labeled ranges, pre- and post-event, over which the S and N_{FI} values were calculated using ssNPA and NBI(SS) data.
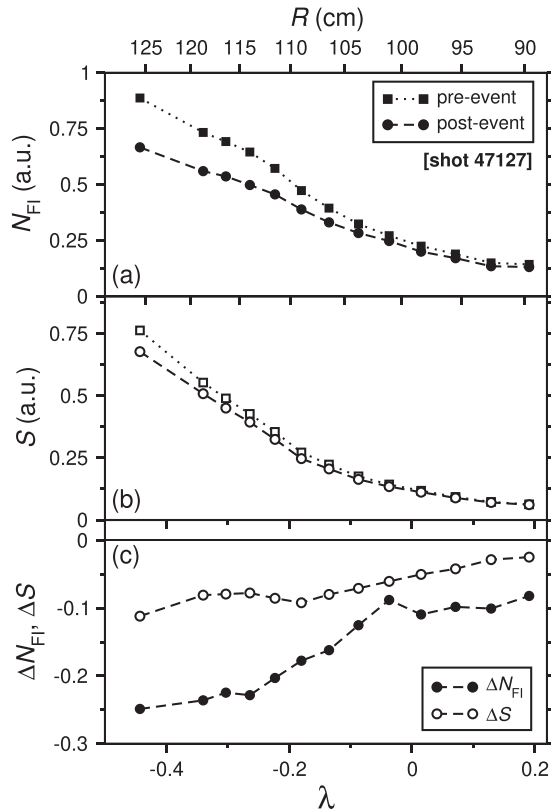
FIG. 7. Comparison of fast-ion population densities, N_{FI} (a), and total ssNPA signals, S (b), measured preceding and following a sawtooth event (t = 387 ms) identified in MAST-U shot 47 127, shown as a function of pitch, λ, and major radius, R. Panel (c) gives the proportional changes in the respective quantities following the event.

neutron rate, produced following the D–D fusion reaction, is also typically associated with sawteeth. This is illustrated in Fig. 6(a), which shows the neutron rates measured in the fission-chamber diagnostic.[11] The NBI(SS) power-output oscillations are shown in panel (b), and panels (c) and (d) show the ssNPA signal, S, at (λ, R) = (−0.443, 125.5 cm) and (−0.087, 103.7 cm), respectively. The approximate time of the sawtooth event, as measured in the ssNPA signals, is indicated by the vertical dashed line. Figure 7 shows N_{FI} (a) and S (b) values as a function of pitch, λ, and major plasma radius, R, both prior to and following the sawtooth event shown in Fig. 6. The relative changes to these respective quantities are then given in panel (c). The pre- and post-sawtooth time ranges over which the data were taken for both N_{FI} and S value measurements are shown in Fig. 6 as dotted vertical lines.

As fast ions are ejected from the plasma during sawteeth, a reduction in the active ssNPA signal would be expected. Their redistribution to the plasma edge will also then lead to an expected increase in passive signal for all lines-of-sight as they interact with the background neutrals concentrated close to the separatrix (midplane $R_{separatrix}$ = 137.9 cm at t = 387 ms for shot 47 127). This is borne out by the present results, which show ΔS shifted above ΔN_{FI} across all (λ, R) values. This is due to S including both active

and passive contributions to the signal, reducing and increasing, respectively, whereas N_{FI} measures the active only.

The utility of the present method is well illustrated in the analysis of the ssNPA time traces in Fig. 6. Oscillations in the signal complicate ΔS measurements, and correcting for δP_{NBI} is not possible as the relative proportions of active, passive, and background signals are not known. Additionally, the countering increase in passive signal makes changes in S difficult to discern [notable in panel (d) at the point of the sawtooth event]. Conversely, changes in N_{FI} are clearly observed through the reduction in amplitude of oscillations of the ssNPA signal between the two ranges, pre- and post-event, relative to those of the NBI(SS).

IV. FUTURE WORK AND SUMMARY

The present method of analysis is applicable also to data from other active diagnostics [such as the Fast-Ion D_α (FIDA) diagnostic[10]] to determine fast-ion distributions as a function of R along the intersecting beamline. Furthermore, refinement of the technique may also be provided by using oscillations in the neutral density along the beamline, which are directly measured using beam-emission spectroscopy to compare with those of the active signal. This would provide a measurement of the beam attenuation as well as a more accurate representation of the neutral-density oscillations at a given position along the beamline.

A method has been developed to determine the fast-ion population density, N_{FI}, in magnetically confined plasmas along a slice of the pitch, λ, major axis, R, variable space using ssNPA-signal, S, and NBI power-output, P_{NBI}, data. Amplitudes of oscillations in the active-CX inducing NBI power output are compared with those reproduced in S, allowing for the active signal component to be separated from those of the passive and background, the active signal being indicative of the $N_{FI}(\lambda, R)$. This method allows for N_{FI} to be measured throughout NBI-heating and is, therefore, particularly useful for measuring changes in fast-ion populations following plasma instabilities. The method uses oscillations in S and P_{NBI} over small signal ranges to determine N_{FI}. This significantly mitigates issues related to detector non-linearity and offsets in signal measurements compared with conventional techniques.

AUTHOR DECLARATIONS

Conflict of Interest

The authors have no conflicts to disclose.

17 January 2024 13:52:57

Author Contributions

E. Parr: Formal analysis (lead); Investigation (equal); Methodology (lead); Writing – original draft (lead). **K. G. McClements**: Conceptualization (equal); Writing – review & editing (equal). **W. W. Heidbrink**: Conceptualization (equal); Investigation (equal); Writing – review & editing (equal). **C. A. Michael**: Investigation (equal); Project administration (equal). **G. Prechel**: Investigation (equal); Writing – review & editing (equal). **J. F. Rivero-Rodriguez**: Investigation (equal); Project administration (equal).

DATA AVAILABILITY

To obtain further information on the data and models underlying this paper please contact PublicationsManager@ukaea.uk.

REFERENCES

[1] K. Shinohara, D. S. Darrow, A. L. Roquemore, S. S. Medley, and F. E. Cecil, Rev. Sci. Instrum. **75**, 3640 (2004).

[2] D. Liu, W. W. Heidbrink, D. S. Darrow, A. L. Roquemore, S. S. Medley, and K. Shinohara, Rev. Sci. Instrum. **77**, 10F113 (2006).

[3] Y. B. Zhu, A. Bortolon, W. W. Heidbrink, S. L. Celle, and A. L. Roquemore, Rev. Sci. Instrum. **83**, 10D304 (2012).

[4] D. Liu, W. W. Heidbrink, K. Tritz, Y. B. Zhu, A. L. Roquemore, and S. S. Medley, Rev. Sci. Instrum. **85**, 11E105 (2014).

[5] Y. B. Zhu, J. Z. Zhang, M. Z. Qi, S. B. Xia, D. Liu, W. W. Heidbrink, B. N. Wan, and J. G. Li, Rev. Sci. Instrum. **85**, 11E107 (2014).

[6] P. A. Schneider, H. Blank, B. Geiger, K. Mank, S. Martinov, F. Ryter, M. Weiland, and A. Weller, "A new compact solid-state neutral particle analyser at ASDEX Upgrade: Setup and physics modeling," Rev. Sci. Instrum. **86**, 073508 (2015).

[7] D. Liu, W. W. Heidbrink, K. Tritz, E. D. Fredrickson, G. Z. Hao, and Y. B. Zhu, Rev. Sci. Instrum. **87**, 11D803 (2016).

[8] J. Z. Zhang, Y. B. Zhu, J. L. Zhao, B. N. Wan, J. G. Li, and W. W. Heidbrink, Rev. Sci. Instrum. **87**, 11D834 (2016).

[9] G. Prechel, N. Fil, D. Liu, W. W. Heidbrink, C. Michael, and A. R. Jackson, MAST-U Team, Rev. Sci. Instrum. **93**, 113517 (2022).

[10] W. W. Heidbrink, Rev. Sci. Instrum. **81**, 10D727 (2010).

[11] C. Vincent, S. Allan, G. Naylor, R. Stephen, S. Bray, A. Thornton, and A. Kirk, Rev. Sci. Instrum. **93**, 093509 (2022).

[12] M. Cecconello, M. Turnyanskiy, S. Conroy, G. Ericsson, E. Ronchi, S. Sangaroon, R. Akers, I. Fitzgerald, A. Cullen, and M. Weiszflog, Rev. Sci. Instrum. **81**, 10D315 (2010).

[13] R. Scannell, M. J. Walsh, M. R. Dunstan, J. Figueiredo, G. Naylor, T. O'Gorman, S. Shibaev, K. J. Gibson, and H. Wilson, Rev. Sci. Instrum. **81**, 10D520 (2010).

[14] J. F. Ziegler, M. Ziegler, and J. Biersack, Nucl. Instrum. Methods Phys. Res., Sect. B **268**, 1818 (2010).

[15] D. Liu, W. Heidbrink, M. Podestà, G. Hao, D. Darrow, E. Fredrickson, and D. Kim, Nucl. Fusion **58**, 082028 (2018).